

**United States
Department of
Agriculture**

**Natural
Resources
Conservation
Service**

**c/o USDA Forest Service
11 Campus Boulevard
Suite 200
Newtown Square, PA 19073
(610) 557-4233; FAX: (610) 557-4200**

Subject: SOI – Ground-penetrating radar study of thaw lake basins,
Barrow, Alaska

Date: 8 June 2001

To: Dr. Wendy Weisner
Associate Professor
Geography Department
712 Swift Hall
University of Cincinnati
P.O. Box 210131
Cincinnati, Ohio 45221-0131

Participants:

Nick Balster, Post Doc, University of Wisconsin, Madison, WI
Jim Bockheim, Professor, University of Wisconsin, Madison, WI
Jim Doolittle, Research Soil Scientist, USDA-NRCS, Newtown Square, PA
John Kimble, Research Soil Scientist, USDA-NRCS, Lincoln, NE
Ken Hinkel, Professor, University of Cincinnati, Cincinnati, OH
Fritz Nelson, Professor, University of Delaware, Newark, DE
Wendy Weisner, Assistant Professor, University of Cincinnati, Cincinnati, OH
Elizabeth Wolfe, Graduate Student, University of Cincinnati, Cincinnati, OH

Activities:

All field activities were completed on 22 to 27 April 2001.

Background:

Thaw lake basins are conspicuous features on the Arctic Coastal Plain near Barrow, Alaska. It is estimated that 50 to 70 percent of the Arctic Coastal Plain is covered by thaw lakes or former thaw lake basins (Hussey and Michelson, 1966). Near Barrow, thaw lake basins form an overlapping and complex pattern with smaller basins often occurring within larger basins. The majority of the thaw lake basins are partially or wholly drained. Basins vary in the shape and morphology. The distinct shapes of thaw lake basins are believed to reflect slow subsidence by thaw, and wind driven wave action and circulation (Carson and Hussey, 1962). Most thaw lake basins have elongated shapes with a common northwest to southeast alignment of their long axes. The long axes of thaw lake basins are related to wave action and water circulation and are at right angle to the prevailing winds, which are from the northeast (Livingstone, 1954). In addition, most thaw lake basins have conspicuous benches on both their upwind and downwind sides (Livingstone, 1954). Carson and Hussey (1962) describe "sublittoral shelves" and "peat bars" on the east and west sides of thaw lakes.

Thaw lake basins reflect the quantity and distribution of ground ice and the susceptibility of soils to thaw and erosion (Hussey and Michelson, 1966). Seasonally ponded water facilitated the formation of thaw lake basins. Accelerated thaw beneath pools of water that occupy the intersection of ice-wedge polygons promotes the development of thaw lakes (Hopkins, 1949). Once formed, these pools of water expand as a result of peripheral thawing and caving.

Ground-ice content and micro-topography of thaw lake basins are believed to change in successive stages of development. With the exception of recently drained lake basins, low-center polygons characterize the surface of

most thaw lake basins (Hussey and Michelson, 1966). In time, ridges form as a result of the upward and lateral movement of expanding ice-wedges that encircle the low center polygons. Relief is about 6 to 18 inches (Hussey and Michelson, 1966).

Based on degrees of vegetation succession and geomorphic development, thaw lakes can be grouped into young, intermediate, old, and ancient aged basins. Young thaw lake basins are characterized by extensive areas of ponded water during summer months. Over time, peat accumulates on the surface of these basins. Massive ice wedges, low-center polygons, and polygon ridges become progressively more pronounced in intermediate- and old-age basins (Bliss and Peterson, 1992; Brown and Krieg, 1983). The increased surface heaving in intermediate- and old-age basins results in drier surface conditions.

The purpose of this investigation was to use ground-penetrating radar (GPR) to investigate the subsurface morphology, map unconformities between underlying lake sediments and post-drainage organic deposits, and determine the thickness of organic deposits within selected, drained thaw lake basins of different ages near Barrow, Alaska.

Equipment:

The radar unit is the Subsurface Interface Radar (SIR)-2000 System, manufactured by Geophysical Survey Systems, Inc.¹ Morey (1974), Doolittle (1987), and Daniels (1996) have discussed the use and operation of GPR. The SIR-2000 System consists of a digital control unit (DC-2) with keypad, VGA video screen, and connector panel. A 12-volt battery powers the system. This unit is backpack portable and, with an antenna, requires two people to operate. As high resolution of shallow subsurface features was required, the comparatively high frequency models 5103 (400 MHz) and 3101D (900 MHz) antennas were used in this study. These antennas were adjusted to provide optimal resolution and penetration depths. The scanning time was 15 nanoseconds (ns) for the 900 MHz antenna and 30 ns for the 400 MHz antenna. The number of scans per minute recorded was 48. All radar profiles have been stored on CD's.

Study Area:

The climate at Barrow is severe with a mean annual temperature of about -12.6°C (Brown, 1967). Annual precipitation is less than 25 cm (Carson and Hussey, 1962). Perennially frozen soils form a continuous blanket over the study area and most of the Arctic Coastal Plain. At Barrow, the thickness of perennial frozen sediments is greater than 300 meters (Brown and Johnson, 1965). The depth of seasonal thaw varies slightly from year to year. Over a period of five years, Brown (1967) observed an average thaw depth of about 38-cm with a range of 33 to 43 cm.

Major soils include Upland Tundra on domes and hummocks, and Meadow Tundra in the troughs of polygonal ground patterns (Brown, 1967). Cryoturbation results in the mixing, disruption and displacement of soil horizons and textural layers (Tarnocai, 1973). Cryoturbation also removes organic materials from surface layers and deposits them within the active layer and along the permafrost table (Mackay et al., 1961). Typically, a thin (0 to 18 cm) organic mat overlays the mineral soil. Within thaw lake basins, the upper part of soil profiles is predominantly silt loam.

Soils contain a large volume of ice as films, lenses, massive layers and large ice wedges. Within the Barrow area, the upper several meters contain about 60 to 70 percent segregated ice by volume (Sellmann and Brown, 1973). Brown (1967) described a typical Meadow Tundra soil profile as having varying concentrations and forms of stratified ice segregations and lenses. Finer ice lenses often occur in the upper part of the mineral soil profile as a result of relatively rapid rates of freezing from the top down (Brown, 1967). In the lower part of the mineral soil profile, thick (5 to 10 cm) horizontal ice lenses develop as a result of the migration and freezing of soil water from the permafrost table up (Brown, 1967).

¹ Manufacturer's names are provided for specific information; use does not constitute endorsement.

While not observed, the dominant vegetation within the study area consists of low, wet tundra (Sellmann and Brown, 1973). Dominant species include sedge (*Carx aquatilis*), grass (*Dupontia fisheri*), and cotton grass (*Eriophorum scheuchzeri* and *Eriophorum angustifolium*) (Brown and Johnson, 1965).

Field Methods:

Fieldwork was carried out in late April, when the active layer was still frozen. At Barrow, this time of the year offers the most favorable temperatures and soil conditions for GPR operations. Active layers inhibit the penetration of radar signals. In thawed medium and fine textured sediments, radar signals are severely attenuated (Arcone and Delaney, 1982). Adsorptive losses (high moisture contents) within the active layer and reflective losses (variable ice and water contents) within the upper part of the permafrost attenuate radar signals. Lawson and others (1998) observed that radar signals suffered less attenuation where the active layer was thin or nonexistent and the permafrost was very close to the soil surface.

At the time of the survey, the study basins were covered by a mantle of snow that averaged about 30 cm and ranged in thickness from 0 to more than 50 cm. Snow cover provided easy access by snowmobiles to the study area with GPR and coring equipment. While this study was being carried out, daytime temperatures ranged from about -10 to 10° F.

In the 1999 study, it was concluded that more appropriate soil information could be obtained by collecting radar data at slower speeds of advance, using faster scan rates, and/or higher frequency antennas. Cryoturbated soil horizons are best expressed on radar profiles when more scans can be collected per unit of time or distance traveled. At least 20 scans are necessary to resolve a subsurface object. The scan rate was increased from 32 (1999 survey) to 48 scans/second. In addition, a higher frequency antenna (900 MHz) was used to improve resolution of subsurface interfaces. The speed of antenna advance across the ground was also reduced.

Greater control was achieved by conducting shorter radar traverses with multiple observation cores to verify interpretations. The degree of interpretative uncertainty increases as the length of radar traverses and the distance between core observations increase. Ground-truth verification is required to confirm the identity and depth to subsurface reflectors. Without these observations false interpretations and unreasonable expectations for GPR can be made. In the absence of sufficient soil coring the identity and depths to most interfaces is more speculative. Even with coring data some uncertainty exist in all interpretations.

Traverse lines were established across twelve thaw lake basins. A series of three, 100-m traverse lines spanned each thaw lake basin in an east to west direction. Along each traverse line, survey flags were inserted in the snow at an interval of 10-m. The SIR-2000 unit was carried in a backpack designed by GSSI and an antenna was pulled by hand along each traverse lines. Each traverse was recorded as a separate file and stored on the hard drive of the SIR2000 unit. The location and length of each radar traverse and the radar file numbers are shown in Table 1. The radar records were printed upon return from the field. These radar records were reviewed and sites were selected for soil coring.

Twelve different thaw lake basins were surveyed. Selection was based upon the inferred age of the thaw lake. Based on photo interpretations each thaw lakes was grouped into one of four age classes: young (Y), Medium (M), Old (O), and Ancient (A). Soil data were obtained from thirty-eight cores collected at specific points along radar traverse lines (see Table 1). A thaw lake basin number, distance along traverse lines as measured from the east end point, and sample number identified cores. Small diameter (6 cm) cores were obtained to depths of ranging from 50 to 164 cm with a *Big-Beaver* drill. Samples were collected by soil horizons and analyzed for moisture content, bulk density, and texture. Core data were compared with radar reflections to verify interpretations.

*Table 1 – Summary of radar file numbers (collected with either the 400 or 900 MHz antennas), file lengths (as measured from the traverse's east end point, and core sample site locations (measured distance and sample number). *Radar traverses conducted first in south to north (File 67), then in a north to south (File 68) directions.*

Thawed Lake Basin	Age	File #		Measured Distance of Lines			Core Sample Locations		
		400 MHz	300 MHz	(M)	(M)	(M)	Meters (sample#)		
B1	M	1-3	4-6	0-100	200-300	400-500	210 (3)	400 (1)	470 (2)
B2	O	7-9	10-12	0-100	135-235	270-370	30 (2)	270 (1)	370 (3)
B3	Y	13-15	16-18	0-100	370-470	740-840	360 (2)	450 (3)	390 (3)
B4	O	19-21	22-24	0-100	300-400	600-700	70 (1)	360 (2)	610 (3)
B5	A	25-27	28-30	0-100	200-300	400-500	200 (1)	300 (2)	410 (3)
B6	O	31-33	34-36	0-90	200-300	410-510	260 (1)	450 (2)	510 (3)
B7	A	37-39	40-42	0-100	216-316	432-532	10 (1)	236 (3)	
B8	Y	43-45	46-48	0-100	252-352	504-604	20 (1)	60 (2)	292 (3)
B9	M	49-51	52-54	0-100	270-370	540-640	20 (1)	290 (2)	580 (3)
B10E	M	55-57	58-60	0-100	200-300	400-500	100 (1)	250 (2)	440 (3)
B10W	M	61-63	64-66	0-100	200-300	400-500	260 (4)	410 (5)	
B11E	O	69-71	72-74	0-100	200-300	400-500	230 (1)	470 (2)	
B11W	O	75-77	78-80	0-100	200-300	400-500	30 (3)	290 (4)	
B11-N	O	82	81	0-200					
B12*	M	67	68	0-200			30 (1)		

Ground-Penetrating Radar:

Ground-penetrating radar is an impulse radar designed for shallow subsurface investigations. It has been used extensively in areas of permafrost. Frozen ground has electrical properties that are favorable to the operation of GPR. Scott and other (1990) observed that as the soil temperature drops below 0°C, the conductivity, dielectric permittivity and loss tangent decrease, while the velocity of propagation increases. As water freezes in soils, penetration depth increases. However, as the amount of ice increases in soils, the contrast in electromagnetic properties between frozen soil layers decreases and the detection of some soil horizons and stratigraphic features with GPR is obscured.

In areas of permafrost, because of the strong contrast in dielectric permittivity between unfrozen and frozen materials, GPR has been extensively used to detect boundaries separating materials containing varying amounts of liquid and frozen water. Ground-penetrating radar has been used to study spatial and temporal variations in the thickness of the active layer (Annan and Davis 1978, Doolittle et al., 1990, 1992, Pilon et al., 1979, 1985, Wong et al., 1977). In addition, GPR has been used to measure dielectric permittivity of frozen sediments (Annan et al., 1975, Annan and Davis, 1976, Davis et al., 1976, Arcone and Delaney 1982, 1984, 1989, Arcone et al., 1982). Ground-penetrating radar has also been used to identify and map areas of massive ground-ice (Arcone et al., 1982, Dallimore and Davis, 1987, Kovacs and Morey, 1979, 1985, Robinson et al., 1993, Scott et al., 1990).

In the 1999 study, identifiable subsurface reflectors observed with a 400 MHz antenna were the permafrost table and ice wedges. The permafrost table appears as continuous, low amplitude, and partially obscured planar reflector. Because of its higher ice content, the approximate long-term position of the permafrost table, though weakly expressed and often partially obscured by reflections from overlying soil interfaces, could be traced laterally across most radar profiles. The low amplitude reflections from the permafrost table were often punctuated by higher amplitude, point reflectors. The point reflectors were interpreted to be ice lenses or the tops of ice wedges. In places, these reflectors were partially obscured by superimposed reflections from overlying horizons. In other places, chaotic patterns or multiple diverging, converging, or overlapping reflections reduced confidence in interpretations.

Cryoturbated soil horizons produced low amplitude, discontinuous, and poorly expressed reflections. Because of their disrupted and mixed nature, most soil horizons were undetectable on radar profiles obtained with the 400 MHz antenna. Other horizons lacked sufficient contrast in electrical properties or were too closely spaced to be discernible on radar profiles. A discontinuous planar reflector with low to medium amplitudes often occurred above the reflection from the permafrost table. This reflector was believed to represent layers of organic matter accumulation (Oe or Oe/Cg horizon), but this observation was not confirmed.

Calibration:

Ground-penetrating radar is a time scaled system. This system measures the time that it takes electromagnetic energy to travel from an antenna to an interface (i.e., soil horizon, stratigraphic layer) and back. In a similar study conducted at Barrow in early May of 1999, the average velocity of propagation was 0.13 m/ns. The velocity of propagation and two-way, pulse travel time are used to depth scale radar profiles. The relationships among depth (d), two-way, pulse travel time (t) and velocity of propagation (v), are described in the following equation (after Morey, 1974):

$$d = vt/2 \quad [1]$$

A conclusion of this earlier study was that the antenna frequency needed to be increased in order to improve the resolution of subsurface features and confidence in interpretations. In general, higher frequency antennas provide greater resolution of subsurface features. Higher frequency antennas have shorter wavelengths and are able to discriminate more closely spaced interfaces than lower frequency antennas. The 400 and 900 MHz antennas were used in this study. Equation [1] and a velocity of 0.13m/ns were used to scale all radar profiles. Davis and Annan (1989) noted that for frequency between 10 to 1000 MHz and at soil conductivities less than 100 mS/m, the velocity of propagation remains constant. These researchers noted that at higher frequencies (>1000 MHz), the velocity of propagation through a medium will increase because of relaxation of water molecules.

Radar interpretations were confirmed with measurements obtained in thirty-eight soil cores. A large number of closely spaced soil horizons were observed in the upper meter of core samples. These horizons were not adequately resolved with the 400 MHz antenna (see Figure 1). On radar profiles, reflections from interfaces spaced closer than one half wavelength apart are indistinguishable due to constructive and destructive interference (Daniels, 1996). Daniels (1996) used the following equation to show the relationship between velocity of propagation (v), antenna center frequency (f), and wavelength (λ):

$$\lambda = v/f \quad [2]$$

Equation [2] shows that the propagated wavelength will decrease with decreasing propagation velocity and increasing antenna frequency. Using equation [2] and an average velocity of 0.13 m/ns resulted in wavelengths of about 35 and 15 cm at frequencies of 400 and 900 MHz, respectively. Compared with the 400 MHz antenna, the 900 MHz antenna had over a twofold increase in resolution.

Interpretation of Radar Profiles:

Figures 1 and 2 are representative radar profile collected along the same portion of a traverse line with the 400 and 900 MHz antennas, respectively. In each profile, the horizontal scale represents units of distance and is expressed in meters. The short vertical lines at the top of the radar profiles represents equally spaced flagged observation points. In each figure, the distance between observation points is 10 meter. In each profile, the vertical scale is a time scale expressed in nanoseconds (ns). Two time scales were used: 30 ns for the 400 MHz antenna, and 15 ns for the 900 MHz.

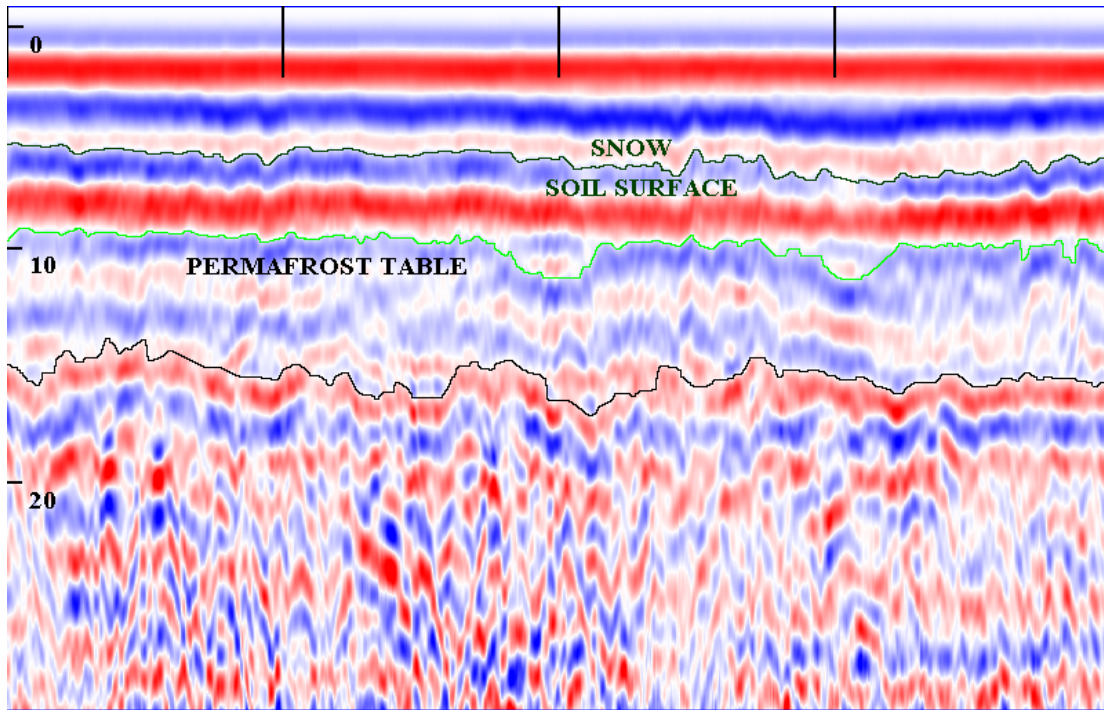


Figure 1 – Representative radar profile collected with a 400 MHz antenna. Depth scale is in nanoseconds. Vertical marks at the top of the radar profile are spaced 10 meters apart. Planar reflectors identified include the snow/ground surface interface, the permafrost table, and an underlying, unidentified discontinuity.

The radar profiles shown in figures 1 and 2 have been processed through the WINRAD software package. Processing was limited to signal stacking, color transforms, and distance normalization. Signal stacking averages several scans and presents the results as a signal trace. Stacking helps to remove unwanted background noise. As the raw data contained a large number of low amplitude reflections, a color transform was used to enhance these reflections. Color transforms resulted in the enhancement of low amplitude reflections with only a minimal effect on high amplitude reflections. Distance normalization corrects for variation in survey speed by stretching and skipping scans between the observation points. Distance normalization provides a uniform horizontal scale.

Although collected from the same portion of a radar traverse, the profiles shown in figures 1 and 2 look dissimilar. Differences in wavelength, elliptical cones of radiation, resolution, and signal amplification have produced seemingly dissimilar imagery. In both figures, the three, continuous horizontal bands at the top of the radar profile represent the snow surface. Differences in color (blue and red) reflect differences in the polarity (either positive or negative) of the signal. The next series of high amplitude reflections immediately below these bands represent the snow/ground surface interface. In both figures, the soil surface has been highlighted with a dark line. With the 400 MHz antenna (see Figure 1), this interface appears to be partially obscured by reflections from the snow surface. With the improved resolution of the 900 MHz antenna (see Figure 2), this interface is well expressed and not obscured.

Below the reflections from the snow/ground interface, subsurface reflections are evident in both radar profiles. The upper part of the radar profile collected with the 400 MHz antenna contains overlapping reflections from several closely spaced interfaces. Individual interfaces are indistinguishable because of inadequate resolution and the occurrence of multiple, closely spaced, often overlapping or superimposed reflections (reverberations) from overlying reflectors. These overlying reflectors produced unwanted clutter that obscured the reflection from the permafrost table. In Figure 1, though highly obscured, the most probable location or reflection from the permafrost table have been identified with a green line. Because of the poor quality of the radar imagery, confidence in this interpretation is exceedingly low.

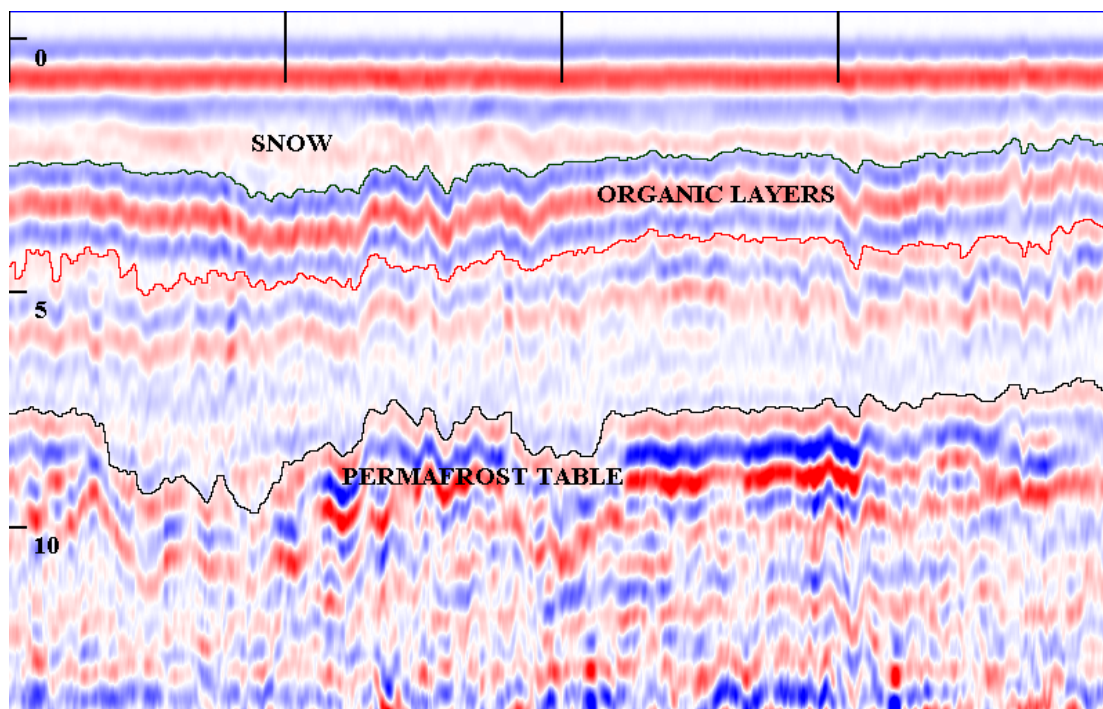


Figure 2 – Representative radar profile collected with a 900 MHz antenna. Depth scale is in nanoseconds. Vertical marks at the top of the radar profile are spaced 10 meters apart. Planar reflectors identified include the snow/ground surface interface, organic/mineral soil interface, and the permafrost table.

A subsurface interface has been identified and traced laterally at a depth of about 1 meter (15 ns) in Figure 1. The interface has been highlighted with a dark line and is characterized by bands of high amplitude planar reflections. This interface separates an over-lying section of low amplitude, superimpose planar reflections from a lower-lying section consisting of multiple, high amplitude point reflections. This interface is believed to represent a stratigraphic discontinuity. The chaotic pattern in the lower portion of this profile may be indicative of the poorly sorted, reworked sediments described by Murton (1996). The low amplitude, superimposed planar reflectors of the upper portion may represent the organic-rich clastic sediments that were laid down in closely spaced, sub-parallel beds. Murton (1996) observed that these sediments are often interbedded with coarser textured sediments. However, it is equally possible that areas with multiple, high amplitude, point reflections extend above this interface and that their reflections have been obscured by the planar, multiple reflections from near surface horizons and layers.

Compared with the 400 MHz antenna, the higher frequency, 900 MHz antenna provides more highly resolved images of near-surface (10 to 80 cm) interfaces. Three easily identifiable interfaces have been traced laterally across the radar profile collected with the 900 MHz antenna (Figure 2). Immediately below the reflection from the soil surface, a very faint, series of continuous reflections is apparent in Figure 2. This reflector occurs at a depth of about 26 to 32 cm (4 to 5 ns). This series of reflections was easily identified and traced on all radar profiles. In many areas, these reflections mimic the reflections from the soil surface. However, in other areas, their patterns and spacing departs from the soil surface's reflections. This shallow, weakly expressed reflection is believed to represent the organic/mineral soil interface.

The permafrost table has been highlighted and labeled in Figure 2. Because of seasonal thawing, water migrates and accumulates at the permafrost table. The permafrost table is detectable because of its greater ice content. The permafrost table contrasts with overlying horizons in ice and moisture contents. In Figure 2, reflections from the permafrost table consist of two or three continuous, horizontal bands. The permafrost table occurs at a depth of about 50 cm (7.5 ns) and can be traced laterally across this figure. Below the permafrost table, several weakly

expressed planar reflections can be traced laterally across the radar profile. In addition, several point reflectors believed to represent ice wedges or lenses, are also apparent in the lower part of the radar profile.

Correlation of radar interpretation with core data:

Soil cores were collected at thirty-eight observation sites. Radar profiles collected with the 900 MHz antenna were scaled, interpreted, and the depth to the organic/mineral soil interface and the permafrost table at each core site were estimated based on equation [1]. Slight spatial discrepancies existed between the core site and the referenced location on the radar profile. The interpreted and measured depths to the organic/mineral soil interface and the permafrost table were compared. At some observation points the organic layers were too thin or were not present (A or AC horizons rather than O horizons). At other observation points the permafrost table was too faint or obscured by closely spaced subsurface layers. The data collected at these observation points were discarded and no interpretations were made.

Table 2 – Comparison of measured and interpreted depths to the organic/mineral soil interface at numbered coring sites within thaw lake basins. All measurements are in cm.

Depths (cm)				
Basin	Obs. #	Measured	Interpreted	Residual
B1	2	14	14	0
B1	3	15	13	2
B2	1	15	16	1
B2	2	13	14	1
B2	3	27	36	9
B3	2	14	10	4
B3	3	24	18	6
B4	1	13	14	1
B4	2	17	19	2
B4	3	20	16	4
B5	1	12	12	0
B5	2	12	13	1
B5	3	12	15	3
B6	1	14	13	1
B6	2	14	13	1
B6	3	13	13	0
B8	3	18	16	2
B9	2	16	14	2
B9	3	20	20	0
B10E	3	13	16	3
B10E	4	20	13	4
BIOW	1	16	20	4
B11E	2	12	13	1

Table 2 summarizes the interpreted and measured depths to the organic/mineral interface or the thickness of the organic layers. The thickness of the organic layers observed in twenty-three soil cores was thin and relatively invariable in depth. At the twenty-three evaluated core sites, the measured depth to the organic/mineral interface observed on soil cores was 15.8 cm with a range of 12 to 27 cm. One half of the observations had measured depths to the organic/mineral interface between 13 and 17.5 cm. At the twenty-three evaluated core sites, the depth to the organic/mineral interface interpreted from the radar profiles was 15.7 cm with a range of 10 to 36 cm. One half of the observations had interpreted depths to the organic/mineral interface between 13 and 16 cm.

The correlation (r) between interpreted and measured depths to the organic/mineral interface was 0.747 (significance level of 0.001). The average difference between measured and interpreted depths to the organic/mineral interface was 2.3 cm with a range of 0 to 9 cm. At one half of these observation sites the

difference was between 1 and 3.5 cm. The match between interpreted and measured depths to the organic/mineral soil interface was considered good.

Table 3 summarizes the interpreted and measured depths to the permafrost table. Compared with the organic/mineral soil materials interface, the permafrost table was deeper and more variable in depth. At twenty-four evaluated core sites, the measured depth to the permafrost table observed on soil cores was 37.7 cm with a range of 26 to 46 cm. One half of the observations had depths to the permafrost table between 34.5 and 40.3 cm. At these same core sites, the depth to the permafrost table interpreted from the radar profiles averaged 37.6 cm with a range of 29 to 49 cm. One half of the observations had interpreted depths to the permafrost table between 33 and 42 cm.

The correlation (r) between interpreted and measured depths to the permafrost table was 0.624 (significance level of 0.001). At these sites, the average difference between measured and interpreted depths to the organic/mineral interface was 3.5 cm with a range of 0 to 9 cm. At one half of these observation sites the difference was between 1 and 6 cm.

Table 3 – Comparison of measured and interpreted depths to the permafrost table at numbered coring sites within thaw lake basins. All measurements are in cm.

Depths (cm)				
Basin	Obs. #	Measured	Interpreted	Residual
B1	1	32	30	2
B1	2	37	31	6
B1	3	32	33	1
B2	1	43	43	0
B2	2	40	40	0
B2	3	40	49	9
B3	3	37	44	7
B4	1	44	35	9
B4	2	39	37	2
B4	3	35	29	6
B6	1	33	29	4
B6	2	37	42	5
B6	3	43	44	1
B7	2	43	42	1
B8	3	38	39	1
B9	2	33	38	5
B9	3	41	41	0
B10E	1	36	38	2
B10E	2	40	39	1
B10E	3	30	29	1
B10W	4	40	33	7
B11E	1	46	42	4
B11E	2	39	42	3
B12	1	26	33	7

Thickness of Organic Soil Materials:

With the 900 MHz antenna, reflections from the organic/mineral soil material interface were low amplitude, but generally clear, continuous, and readily identifiable. At each observation point on the radar profiles, the thickness of the surface organic materials was determined. The smallest thickness detectable with the 900 MHz antenna was about 8 cm. At all observation points having surface organic materials thin to be measure with the 900 MHz antenna, the thickness was recorded as 7.6 cm. At these observation points the actual thickness of the organic layers could range from 0 to 7.6 cm. Within the selected thaw lake basins, the thickness of surface organic materials was thin and relatively invariable. Based on 385 GPR measurements, the interpreted thickness of the

surface organic materials averaged 14.8 cm, with a range of 7.6 to 33.1 cm. One half of the observations had surface organic materials between 11.1 and 17.8 cm thick.

The twelve basins were grouped into four age sets. An analysis of variance revealed no significant difference in average thickness of surface organic soil materials among basins grouped into four different age classes (F-value 0.716).

Table 4 – Summary of interpreted thickness of organic soil materials in twelve basins. Basins are distinguished by age: Y = Young; M = moderate; O = old; and A = Ancient. All statistics are in cm.

Basin	Age	OBS.	Average	Minimum	Maximum	SD	First	Third
1	M	33	15.2	12.7	22.9	2.4	14.0	16.5
2	O	33	14.8	10.2	21.6	3.1	3.1	12.7
3	Y	33	13.0	7.6	19.1	3.3	10.2	15.3
4	O	33	15.5	7.6	25.5	3.5	14.0	17.8
5	A	33	12.9	8.9	16.5	2.0	11.5	14.0
6	O	28	14.5	10.2	17.8	2.2	12.7	15.3
7	A	33	14.4	10.2	22.9	3.5	11.5	16.5
8	Y	22	16.3	10.2	33.1	5.3	13.0	17.8
9	M	33	15.3	10.2	21.6	3.3	12.7	17.8
10	M	66	12.7	8.9	20.4	2.5	10.2	14.0
11	O	17	17.0	10.2	25.5	3.9	15.3	20.4
12	M	21	15.9	12.7	21.6	2.5	14.0	16.5

Conclusions:

Ground-penetrating radar can provide a wealth of interpretive information. In most soil investigations, a small number of orderly arranged, continuous, and contrasting soil horizons simplifies radar interpretations and drastically reduces the number of cores required to verify interpretations. Radar interpretations are more obscured in areas of Gelisols. Areas of cryoturbated soils are generally unfavorable for the interpretation of radar data. Because of cryoturbation, soil horizons are often closely spaced, mixed and discontinuous. Interpretation errors often occur where two or more interfaces are close together. In some instances a reflector can appear to split into two interfaces. In other instances, two closely spaced reflectors can appear to merge into one reflector. In these cases, interpretations are considered less reliable. Additional coring is often required to allay the uncertainty and confirm interpretations.

The 900 MHz antenna greatly improved the resolution of near surface (0 to 80 cm) soil interfaces and increased confidence in radar interpretations. Two subsurface interfaces, the organic/mineral soil interface and the permafrost table, were identified and traced laterally across all radar profiles. A strong ($r = 0.747$) and significant (0.001 level) correlation was found between interpreted and measured depths to the organic/mineral soil interface at 23 core sites. A slightly weaker ($r = 0.624$), but still significant (0.001 level) correlation was found between interpreted and measured depths to the permafrost table at 24 core sites. The thickness of the surface organic soil materials was interpreted at 385 observation points located in twelve thaw lake basins. The interpreted thickness of the surface organic soil materials averaged 14.8 cm, with a range of 7.6 to 33.1 cm. These interpretations closely agreed with measurements taken at 38 core sites located in these thaw lake basins.

Prior to the use of GPR, the twelve surveyed thaw lake basins were grouped into four age classes (young, medium, old, and agent) based on photo interpretations, surface vegetation and morphology. Acquired GPR data on the thickness of the organic layers were grouped according to the ages of the thaw lake basins. An analysis of variance of the average thickness of surface organic soil materials revealed no significant difference among the basins. Basins of different ages have similar thickness of surface organic soil materials. It is inferred from these results that, in this environment, organic materials accumulate until a threshold thickness is achieved. Once this threshold thickness is achieved, further accumulations are restricted and become relatively stagnant. Drier surface conditions resulting from increased surface heaving or increased cryoturbation may be responsible for the apparent stagnation of peat accumulation with increased age of thaw lake basins.

At Barrow, thaw lake basins are remote and relatively inaccessible during the summer months when the soil has thawed. During winter months, the soil is frozen and resists soil probe observations. The use of GPR with a 900 MHz antenna provided a rapid and fairly accurate method to determine the thickness of the surface organic soil layers and the depth to the permafrost table.

With kind regards,

James A. Doolittle
Research Soil Scientist

cc:

- R. Ahrens, Director, USDA-USDA, National Soil Survey Center, Federal Building, Room 152,100 Centennial Mall North, Lincoln, NE 68508-3866
- J. Bockheim, Professor, Department of Soil Science, University of Wisconsin, 1525 Observatory Drive, Madison, WI 53706-1299
- K. Hinkel, Associate professor, Geography Department, 712 Swift Hall, University of Cincinnati, Cincinnati, OH 45221-0131
- J. Kimble, Research Soil Scientist, USDA-USDA, National Soil Survey Center, Federal Building, Room 152,100 Centennial Mall North, Lincoln, NE 68508-3866
- F. Nelson, Professor, Department of Geography, University of Delaware, Newark, DE 19716
- C. Olson, National Leader for Soil Investigations, USDA-USDA, National Soil Survey Center, Federal Building, Room 152,100 Centennial Mall North, Lincoln, NE 68508-3866
- H. Smith, Director of Soils Survey Division, USDA-NRCS, Room 4250 South Building, 14th & Independence Ave. SW, Washington, DC 20250B.

References:

- Annan, A. P. and J. L. Davis. 1976. Impulse radar sounding in permafrost. *Radio Science* 2:383-394.
- Annan, A. P. and J. L. Davis. 1978. High frequency electrical methods in the detection of the freeze-thaw interface. IN: *Proceedings of the Third International Conference on Permafrost*. Edmonton, Alberta. National Research Council of Canada, Ottawa. 495-500.
- Annan, A. P., J. L. Davis, and W. J. Scott. 1975. Impulse radar wide-angle reflection and refraction sounding in permafrost. *Geological Survey of Canada Paper 75-1C*: 335-341.
- Arcone, S. A. and A. J. Delaney. 1982. Dielectric properties of thawed active layers overlying permafrost using radar at VHF. *Radio Science* 17(3): 618-626.
- Arcone, S. A. and A. J. Delaney. 1984. Radar investigations above the Trans-Alaskan Pipeline near Fairbanks. U. S. Army Cold Regions Research and Engineering Laboratory, CRREL Report 84-27. 15 p.
- Arcone, S. A. and A. J. Delaney. 1989. Investigation of dielectric properties of some frozen materials using cross-borehole radiowave pulse transmission. CRREL Report 89-4. 16p.

- Arcone, S. A., P. V. Sellmann, and A. J. Delaney. 1982. Radar detection of ice wedges in Alaska. U. S. Army Cold Regions Research and Engineering Laboratory, CRREL Report 82-43. 15 p.
- Bliss, L. C., and Peterson, K. M. 1992. Plant Succession, Competition, and the Physiological Constraints of Species in the Arctic. *In* "Arctic Ecosystems in a Changing Climate: An ecophysiological perspective." (F. S. Chapin, R. L. Jefferies, J. F. Reynolds, G. R. Shaver, and J. Svoboda, Eds.), pp. 111-136. Academic Press, San Diego, CA.
- Brown, J. 1967. Tundra soils formed over ice wedges, northern Alaska. *Soil Sci. Soc. America Proc.* 31: 686-691.
- Brown, J., and P. L. Johnson. 1965. Pedo-ecological investigations, Barrow, Alaska. U. S. Army Cold Regions Research and Engineering Laboratory, CRREL Technical Report 159. 32 p.
- Brown, J., and Krieg, R. A. 1983. "Guidebook to Permafrost and Related Features." Alaska Geological and Geophysical Surveys, College, AK.
- Carson, C. E. and K. M. Hussey. 1962. The oriented lakes of arctic Alaska. *Journal of Geology* 70: 417-439.
- Dallimore, S. R. and J. L. Davis. 1987. Ground-probing radar investigations of massive ground ice and near surface geology in continuous permafrost. *Current Research, Part A. Geological Survey of Canada Paper 87-1A*: 913-918.
- Daniels, D. J. 1996. *Surface-Penetrating Radar*. The Institute of Electrical Engineers, London, United Kingdom. 300 p.
- Davis, J. L., and A. P. Annan. 1989. Ground-penetrating radar for high resolution mapping of soil and rock stratigraphy. *Geophysical Prospecting* 37: 531-551.
- Davis, J. L., W. J. Scott, R. M. Morey, and A. P. Annan. 1976. Impulse radar experiment on permafrost near Tuktoyaktuk, Northwest Territories. *Canadian Journal of Earth Science* 13:1584-1590.
- Doolittle, J. A. 1987. Using ground-penetrating radar to increase the quality and efficiency of soil surveys. 11-32 pp. *In*: Reybold, W. U. and G. W. Peterson (eds.) *Soil Survey Techniques*, Soil Science Society of America. Special Publication No. 20. 98 p.
- Doolittle, J. A., M. A. Hardisky, and S. Black. 1992. A ground-penetrating radar study of Goodream Palsen, Newfoundland, Canada. *Arctic and Alpine Research* 24(2):173-178.
- Doolittle, J. A., M. A. Hardisky, and M. F. Gross. 1990. A ground-penetrating radar study of active layer thicknesses in areas of moist sedge and wet sedge tundra near Bethel, Alaska, U.S.A. *Arctic and Alpine Research* 22(2): 175-182.
- Hinkel, K. M., J. Doolittle, J. Bockheim, F. E. Nelson, R. Paetzold, J. Kimble, and R. Travis. 2001. Preliminary Study of Subsurface Features Using Ground-Penetrating Radar at Barrow, Alaska. *Permafrost and Periglacial Processes*. 12 (2) :(In preparation).
- Hopkins, D. M. 1949. Thaw lakes and thaw sinks in the Imuruk Lake Area, Seward Peninsula, Alaska. *Journal of Geology* 57:119-131.
- Hussey, K. M. and R. W. Michelson. 1966. Tundra relief features near Point Barrow, Alaska. *Arctic* 19:162-184.
- Kovacs, A. and R. M. Morey. 1979. Remote detection of massive ice in permafrost along the Alyeska pipeline and the pump station feeder gas pipeline. 268-279 pp. *IN: Proceedings of the Specialty Conference on Pipelines in Adverse Environments*. American Society of Civil Engineers. New Orleans, Louisiana, 15-17 January 1979.
- Kovacs, A. and R. M. Morey. 1985. Impulse radar sounding of frozen ground. 28-40 pp. *IN: Brown, J., M. C. Metz, and P. Hoekstra (Eds.). Workshop on Permafrost Geophysics, Golden, Colorado, 23-24 October 1984*. U. S. Army Cold Regions Research and Engineering Laboratory, Special Report 85-5.

- Lawson, D. E., S. A. Arcone, A. J. Delaney, J. D. Strasser, J. C. Strasser, C. R. Williams, and T. J. Hall. 1998. Geological and geophysical investigations of hydrogeology of Fort Wainwright, Alaska. U. S. Army Cold Regions Research and Engineering Laboratory, Report 98-6. 66 p.
- Livingstone, D. A. 1954. On the orientation of lake basins. *American J. of Science* 252:547-554.
- Mackay, J. R., W. H. Mathews, and R. S. MacNeish. 1961. Geology of the Engigstciak archaeological site, Yukon Territory. *Arctic* 14: 25-52.
- Morey, R. M. 1974. Continuous subsurface profiling by impulse radar. 212-232 pp. In: Proceedings, ASCE Engineering Foundation Conference on Subsurface Exploration for Underground Excavations and Heavy Construction, held at Henniker, New Hampshire. Aug. 11-16, 1974.
- Murton, J. B. 1996. Thermokarst-lake basin sediments, Tuktoyaktuk Coastlands, western arctic Canada. *Sedimentology* 43:737-760.
- Pilon, J. A., A. P. Annan, J. L. Davis, and J. T. Gray. 1979. Comparison of thermal and radar active layer measurements in the Leaf Bay Area, Nouveau-Quebec. *Geographie Physique et Quaternaire* 23: 317-326.
- Pilon, J. A., A. P. Annan, and J. L. Davis. 1985. Monitoring permafrost ground conditions with ground probing radar (G.P.R.) 71-73 pp. IN: Brown, J., M. C. Metz, and P. Hoekstra (eds.). Workshop on Permafrost Geophysics, Golden, Colorado, 23-24 October 1984. U. S. Army Cold Regions Research and Engineering Laboratory, Special Report 85-5.
- Robinson, S. D., B. J. Moorman, A. S. Judge, and S. R. Dallimore. 1993. The characterization of massive ice at Yaya Lake, Northwest Territories using radar stratigraphy techniques. p. 23-32. IN: Current Research, Part B. Geological Survey of Canada, Paper 93-1B.
- Scott, W. J., P. Sellmann, and J. A. Hunter. 1990. Geophysics in the study of permafrost. 355-384 pp. IN: Geotechnical and Environmental Geophysics, Vol. 1: Review and Tutorial. Society of Exploration Geophysicists Investigation in Geophysics, No. 5.
- Sellmann, P. V., and J. Brown. 1973. Stratigraphy and diagenesis of perennially frozen sediments in the Barrow, Alaska, region. 171-181 pp. IN: Permafrost: North American Contribution to the Second International Conference. Washington, National Academy of Sciences.
- Tarnocai, C. 1973. Soils of the Mackenzie River area. Task Force on Northern Oil Development, Report 73-26. Info. Canada Cat. No. R72-9673. 136 pp.
- Wong, J., J. R. Rossiter, G. R. Olhoeft, and D. W. Strangway. 1977. Permafrost: electrical properties of the active layer *in situ*. *Canadian Journal of Earth Science* 14(4): 582-586.

: